

MOBILE DATA ACQUISITION AND PROCESSING IN SUPPORT OF AN URBAN HEAT ISLAND STUDY

R. Zeynali¹, G. Bitelli¹, E. Mandanici^{1*}

¹ Department of Civil, Chemical, Environmental and Materials Engineering, University of Bologna, Viale del Risorgimento 2, 40136 Bologna, Italy – (reyhaneh.zeynali2, gabriele.bitelli, emanuele.mandanici)@unibo.it

KEY WORDS: Urban Heat Island Effect, Urban Microclimate, Interpolation Models, Mobile Mapping, Bologna

ABSTRACT:

Global warming and changes in Earth's weather patterns are the main consequences of climate change, and bioclimate discomfort has significant public health problems, especially for the elderly. Normally, the thermal characteristics of urban areas are poor due to a phenomenon known as urban heat island. Mobile and fixed temperature measurements were performed on 19 March 2021 in the city of Bologna, Italy. Mobile measurements took place with a car, along a 75-km transect, starting at 22:16 with a duration of 2 hours and 41 minutes, while fixed measurements were done using 15 present weather stations and also placing five thermometers in the city center. Various interpolation models (i.e., Traditional, Voronoi Tessellation, Global Trends, Triangulated Irregular Networks, Inverse Distance Weighting and Kriging) were applied to correct the mobile measurements using fixed data. Kriging fulfilled the best result with a correlation coefficient of 0.99 compared to the raw temperatures.

1. INTRODUCTION

Climate change is predicted to increase the average temperature of the Earth, and according to the Intergovernmental Panel on Climate Change (IPCC: 2013) the near-surface global temperature will increase by 0.4-2.6 °C (Georgiadis, 2017). Furthermore, the population of the cities is increasing, and it is forecasted that two-thirds of the world population will live in cities by 2050 (Nardino et al., 2021). By considering this, it is essential to properly estimate the risks associated with it and to designate appropriate strategies to reduce people's vulnerability. It is well known that the rise of air temperature has a higher impact on the elderly and children. Italy has the highest proportion of elderly in Europe. 29.4% of its population was over 60 years old in 2017, and it is projected to reach 40.3% by 2050 (Nardino et al., 2021). Therefore, it makes thermal and microclimate studies even more crucial for the country. Another issue is that different parts of a city have different thermal regimes and consequently different impacts on citizens (Declet-Barreto et al., 2016). Hence, there is a strong need of knowing the microclimate of the city to define and apply strategies and actions.

The city's local climate is affected by its own structure and composition as well as large-scale meteorological phenomena. The term of urban heat island (UHI) comes from the fact that the local temperature of an urban area is considerably higher than its neighboring rural area (Oke, 1982). It is reported a yearly average of approximately 1 to 2°C higher temperature in a large city compared to its surrounding rural area. Furthermore, it is proved that this difference will reach up to 12°C on calm and clear nights (Georgiadis, 2017). The variance of UHI is variable and depends on land cover/use patterns (e.g., impervious surface, vegetation, water, buildings, and bare soil), seasons, and day/night (Deilami et al., 2018). Its main contributor is urban growth which results in the change of land cover from pervious surfaces to artificial impervious ones (i.e., most urban materials are dark which trap heat, and have low permeability with reduced ability to dissipate the heat because of sparse pores to store moisture). It is reported that impervious surfaces explain around 70% of the total land surface temperature variance in the 38 most populated cities in the US (Imhoff et al., 2010). Seasonal variation is another factor that

impacts the intensity of UHI. Solar radiation reaching the earth's surface and also metabolic activity of vegetation varies in different seasons. As a result, UHI is varied and usually is higher in spring and summer than in autumn and winter. Seasonal variation in UHI is also affected by geographical location. For instance, it is showed that there is no UHI intensity during the summer in Cairo (Taheri Shahraini et al., 2016). Generally, its intensity is much less when a city is located in an arid or semiarid climate (Deilami et al., 2018). UHI exists at any time of day and night, but its intensity is higher during the night-time. Because of the high thermal capacity of urban materials, the cooling process of the city center after sunset is slower than of suburbs (Haashemi et al., 2016).

In general, UHI worsen urban microclimate. Taking into account the urban microclimate can strongly improve the urban policies, such as buildings regulation, and help to speed up the sustainable and resilient development of a city (Bitelli et al., 2020). Accordingly, the development of different measurement methods to have a clearer view in time and space of the urban thermal environment is crucial. The main threat for the next generation is climate change in this regard. Therefore, more ambitious, and broad goals for climate and energy are set by the Covenant of Mayors. These goals are considering not only climate change mitigation but also adaptation (Ventura et al., 2010). Bologna is the first Italian town adopting the new goals and adaptation plans that are presented by the Covenant of Mayors, and it performed enormous number of thermal studies (Nardino et al., 2021; Zauli Sajani et al., 2008).

Different strategies have been developed to determine UHI. In-situ is the most frequent approach which are divided into two categories, fixed and mobile measurement. For the fixed measurement, data are collected from some meteorological stations (fixed campaigns) placed in different areas of the city and within the atmospheric layer (Bahi et al., 2020). These stations are permanently installed to provide data on a daily, weekly, seasonal, or annual basis, and they are not implemented solely to measure air temperature but also to study other problems such as dispersion of air pollution and vertical air temperature profile. Widespread weather private stations, able to provide online temperature time series, could be also adopted, but the inhomogeneity in their realization and

placement gives little guarantee on their massive use without a careful selection. On the other hand, for the mobile measurement, a traveling path within the urban area is defined and then the thermal data are obtained on foot or by using a means of transport like a bicycle or a car. The applied sensors should be protected from the vehicle exhaust heat and temperature changes along the travel path, and the temperature measurements should be corrected by selecting the same endpoint as the start point. It can be carried out at any time with high spatial density (Imhoff et al., 2010). Therefore, it allows access to a large part of the urban area, and it theoretically can cover all the city streets. However, when a single sensor is used, this approach cannot measure temperature simultaneously at different positions. To overcome this problem, data from mobile measurement should be adjusted temporally with the help of reference temperature measured at the start and endpoint of the path. Another way could be to use more mobile sensors, but the operational cost will increase (Imhoff et al., 2010). Using data acquired from satellite sensors and remote sensing is another way of measuring UHI, and they may be coupled with geomatic methods for geometric urban 3D modeling (Bitelli et al., 2018; Africani et al., 2013). However, measurements in some urban parts are dismissed from remote sensing, such as the covered area with plant canopy, vertical surfaces, and walls. Therefore, ground observations are required to modify the true temperature of 3D surfaces. Another limitation is the lack of continuous information records over a daily period, depending on the characteristics of the spatial missions. Lastly, computer modeling can be applied to simulate the thermal spatial distribution and energy flow in the urbanized area to analyze the UHI phenomenon. This approach is a way to overcome the limitation of the fixed in-situ measures (Bahi et al., 2020).

The main objective of this study is to propose a methodology for the temporal adjustment of the temperature data acquired with a car along a transect, using the logs of a limited number of weather stations sparse in the city; the nocturnal temperature changes (since these changes are much more obvious during the night) in the city center of Bologna compared to its suburbs are also measured. The results can help understanding the different thermal regions of Bologna to support the city's development strategies and microclimate adaptation.

2. MATERIALS AND METHODS

2.1 The Study Area

The survey is done in the city of Bologna, on the 19 March 2021. With about 400,000 inhabitants and 150 different nationalities, Bologna is the capital and largest city of the Emilia Romagna region in northern Italy, ($44.4949^{\circ} N$; $11.3426^{\circ} E$) (Ventura et al., 2010). Its urban area covers about 60 km^2 (Zauli Sajani et al., 2008). It is a meeting point between the north and the south, and between the east and the west of the country. Bologna has a temperate climate, which the monthly average temperature ranges from 3.5°C in January to 25.5°C in July (Nardino et al., 2021). It is an ancient city with particular architecture in the center, which is mainly characterized by a dense pattern of short buildings, remaining from the medieval and renaissance eras, with relatively narrow roads and a high presence of porticoes (Nardino et al., 2021). Conversely, in the peripheral and productive districts a wider variety of modern building types can be found (e.g., industrial sheds and condominiums), and many open spaces are present (Trevisiol et al., 2022). This varying building density may produce different temperature patterns in the districts.

2.2 Data Acquisition

Temperature data are collected from a mobile survey throughout the city and the suburbs, 15 selected online weather stations, and 5 fixed thermometers that were placed in different parts of the city during the experiment. A car equipped with a thermometer (DeltaOhm DO9847 datalogger with probe HP472ACR with an accuracy of $\pm 0.25^{\circ} \text{C}$) on its roof (Figure 1) traveled to measure air temperature and relative humidity. DeltaOhm air temperature probe was chosen since it is faster and more responsive compared to the thermometers used for fixed stations. A multiplate shield (shaped as a Stevenson's screen) was used to protect the thermometer from the wind. The car moved in a predefined path designed to be as representative as possible of the whole area of study. It started from the northeastern part of the city and finished at the same point, after crossing the city center in NE-SW and SE-NO directions. Figure 2 shows the car path while different colors represent raw values of the air temperature. The survey started on 19 March 2021, at 22:16, and finished at 00:57 (total duration of 2 hours and 41 minutes). The average speed of the car was around 28 km/h , traveling approximately 75 km . Data acquisition speed was one temperature record per second.

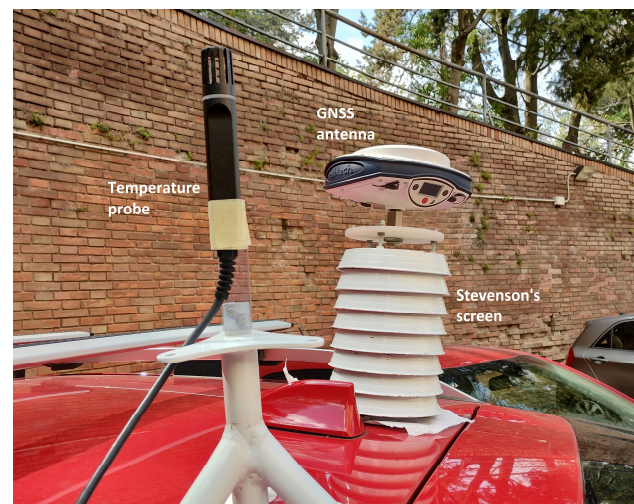


Figure 1. Placement of the thermometer on the car's roof.

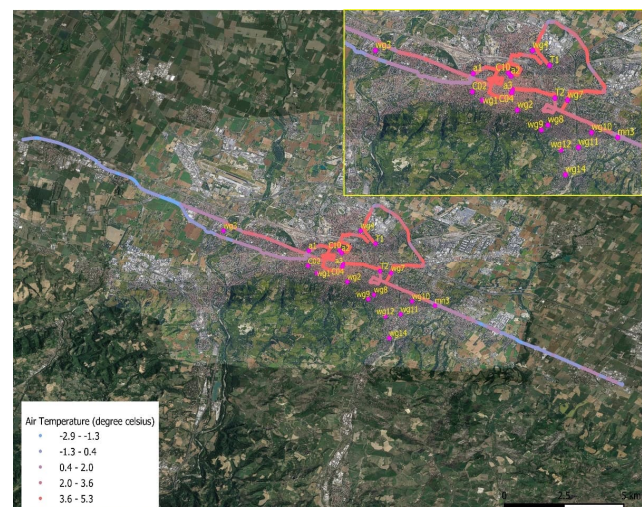


Figure 2. The car path (points colored by the raw temperature values) and positions of the fixed stations.

Two types of fixed stations are used to acquire temperature data. The first group is online weather stations. After finding all the weather stations in the region (total of 49 stations), first, their locations were checked and those which were far from the car transect were deleted. Then, it was checked if they are active and at what time interval they provide temperature data. To do so, the online stations were checked daily for approximately one month (from 13 January to 9 February 2021). Throughout this procedure, some of the stations were removed, and finally, a total of 15 were selected (Figure 2). All the online stations are located at a high elevation above the ground, except for *a1*, *a2*, and *a3* which are placed at 2 meters. Also, for most of the stations, one data is provided every 5 minutes (stations *wg1*, *wg2*, *wg3*, *wg6*, *wg7*, *wg11*, and *wg12*) except for *wg4* and *wg9* (one temperature data every 10 minutes), *wg8* and *wg10* (one temperature data every 15 minutes) and *a2* and *a3* (one temperature data every 30 minutes) and *a1* (one temperature data every hour).

The second group of fixed stations consists of thermometers that was installed manually in different parts of the city. A total number of five thermometers, named *C02*, *C04*, *C10*, *T1*, and *T2*, were placed in the city's urban area on the 19 March 2021 (Figure 2). The first three are of the model Extech RHT10 (with the temperature range from -40 °C to +70 °C, resolution of 0.1 °C, and accuracy of ±1.0 °C) providing temperature data every 60 seconds. Other data acquired are relative humidity and dewpoint. Whereas in *T1* and *T2* two Extech SD200 were used, with a temperature range from -100 °C to +1300 °C, resolution of 0.1 °C and accuracy of ±(0.5% + 0.5 °C). The sampling rate was set to 5 minutes, and also relative humidity and air pressure are measured. Data collection from the fixed stations started on the same day as the car transect, therefore, on the 19 March 2021, between 21:00 and 03:00 (the morning of the next day).

2.3 Data Correction

2.3.1 Traditional Method

The traditional method considers a linear change of the temperature over the traveling path (Equation 1). To calculate the coefficients of equation 1, the temperature range over the transaction path is first determined, which is the difference in temperature measured in the same location at the beginning and the end of the survey (the transect started and ended in the same point). Then, linear equation passing the start and end times is calculated.

$$\Delta T = at + c \quad (1)$$

where ΔT = temperature difference
 t = time

Using equation 1, corrected ΔT and then corrected temperatures are calculated at any time of the survey. With this method, fixed stations are not considered.

2.3.2 Proposed Method

In this method, the regression equations that best describe the data from each of the fixed stations were determined. Three different curves, linear, exponential, and second-degree polynomial were fitted for each station. Since for the majority of the stations, the polynomial regression of degree-two was found the best option to describe the temperature behavior, it is selected as the trend, considering the value of the R-squared

(R^2) and assuming that its higher amount shows a better fit and lower error.

Furthermore, for each fixed station, it was decided to calculate the temperature difference at each measurement point with regard to a reference temperature. The assumed reference was the temperature at the starting point of the mobile transect (at 10:00 PM, 19 March 2021). Therefore, temperature differences for all the data acquired after 10:00 PM are calculated. Then, the second-degree polynomial curve (Equation 2) is fitted to the temperature differences. Figure 3 is an example of the fitted polynomial on the temperature differences over time and for the fixed station *T1*. In this case, a, b, and c coefficients are -48.91, 112.51, and -61.54, respectively.

$$\Delta T = at^2 + bt + c \quad (2)$$

$$T_{corr} = T + \Delta T \quad (3)$$

where

ΔT = temperature difference of fixed stations
 T = raw temperature data from car transect
 T_{corr} = corrected temperature
 t = time

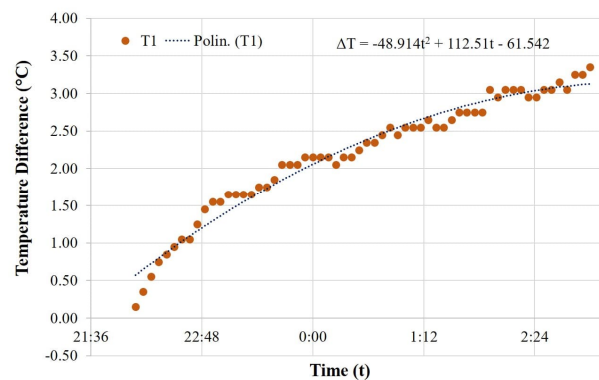


Figure 3. Polynomial second-degree fitted on the temperature differences of the fixed station *T1*.

If the second order polynomial proves to effectively model the trend of temperature decrease during the time span of the survey, then this model can be used to detrend the temperature measured by the car. The problem is that the coefficients of the polynomial vary from station to station and can assume different values in every location. To solve this problem, some advanced interpolation approaches (Voronoi tessellation polygons, trend surface fitting, triangulation irregular networks (TINs), inverse distance weighted (IDW) and Kriging) are tested to map the coefficient of the second order polynomial over the whole area of the city. In other words, different interpolation methods are applied to each coefficient of equation 2. Figure 4 is an example of applying Kriging interpolation on the *a*-coefficient achieved from all the fixed stations. Thanks to the interpolation, the value of *a*-coefficient can be derived for all the transect path. This is done for all the coefficients and applying different interpolation methods. Interpolating these coefficients allows calculating temperature differences along the travelling path, which then are used to derive the corrected temperatures. This is done using Equation 3 and the original temperatures.

To check the effectiveness of the corrections, the correlation between raw mobile data and the corrected ones (using different

interpolation methods) is also computed. The correlation coefficient can be achieved from Equation 4 (Rumsey, 2021).

$$r = \frac{1}{n-1} \left(\frac{\sum X \sum Y (X - \bar{X})(Y - \bar{Y})}{S_X S_Y} \right) \quad (4)$$

where r = correlation coefficient
 n = total number of data in each data set
 X and Y = data from the two data set
 \bar{X} and \bar{Y} = mean value for each data set
 S_X and S_Y = standard deviation for each data set

The correlation coefficient r can have a value between -1 and 1 (where -1 and 1 show strong negative and positive correlations between the two data sets, respectively).

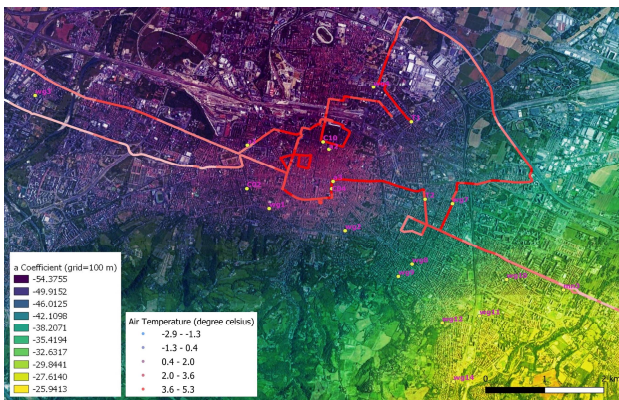


Figure 4. Interpolation of 'a' coefficient over the study area using Kriging.

One method of data interpolation is to define an area of influence for each station by applying Voronoi tessellation polygons. Then, each mobile temperature data is corrected based on the polynomial regression for the station in which it is located. Next method is to find a surface over transect area which describes the behavior of the air temperature data. Then, mobile temperatures can be corrected based on the equation of this surface. To do so, a simple planar surface and a bilinear saddle are firstly created. Then using both surfaces, approximate values of the coefficients (Equation 2) are achieved for each measure of the car transect. Another method that has been applied is TINs. This method creates a network of triangles over the study area and using the coefficients of the second order polynomial regression for the temperature differences (Equation 2). After that, the approximate values of these coefficients and as a result, the corrected temperatures are calculated for each measurement of the car transect. Similar to the previous models, the IDW method was used to interpolate the coefficients of the polynomial regression and to find the corrected temperatures. The last method was Kriging, which, similarly to the previous methods, is applied to the coefficients of Equation 2, and then the corrected thermal data are achieved. The size of the gridding window is very important since small windows tend to exaggerate local extreme values, while large ones have a smoothing effect on the predicted value (Huisman & de By, 2009). Here, cell size is set to 100 m, as a trade-off value, for all the tested interpolation methods.

3. RESULTS AND DISCUSSION

Mobile temperature acquisition happened during the night and took almost three hours to be finished. Normally, during the

night, the air temperature tends to decrease at different rates in different locations. To rectify these various trends, mobile temperatures need to be corrected using a model based on temperature records from the fixed stations. Some of them are close to the car route, i.e. *wg3*, *wg10*, *a3* and *T2*. Table 1 compares the raw temperatures extracted from the transect with the temperatures measured by the stations at the time when the car passed close to them. Sensible differences can be observed, especially for the stations *wg3*, *a3*, and *T2*.

Table 1. Comparison of raw temperature data from mobile and close fixed stations.

| Station | Time | Fixed Temp. | Mobile Temp. | Difference |
|---------|-------|-------------|--------------|------------|
| wg3 | 00:32 | 1.44 | 0.88 | -0.56 |
| a3 | 23:30 | 3.80 | 5.05 | 1.25 |
| T2 | 23:25 | 5.40 | 3.58 | -1.82 |
| wg10 | 23:14 | 2.83 | 2.72 | 0.02 |

The highest temperature difference is observed when the car passed near station *wg3* with an absolute amount of 0.56 °C (39% lower than the quantity which was measured by *wg3* and at 23:25 midnight). The lowest temperature difference of around one percent is observed when the car passed *wg10* (Table 1).

First, the traditional method is applied to correct the mobile temperatures and the result is summarized in Figure 5. This could be used as a framework to validate the other methods of correcting data. The temperature difference between the beginning (mobile temperature at 22:16 was 5.13°C) and the ending point (mobile temperature at 00:57 was 3.72°C) of the survey was -1.41 °C. Considering that the temperature changes linearly over the traveling path, linear Equation 1 is calculated for the data and rewritten as Equation 5. The correlation between the raw and corrected data is calculated to be approximately 98%. This method is acceptable and used widely in the past studies (Bitelli et al., 2020).

$$\Delta T = -12.60 t + 11.69 \quad (5)$$

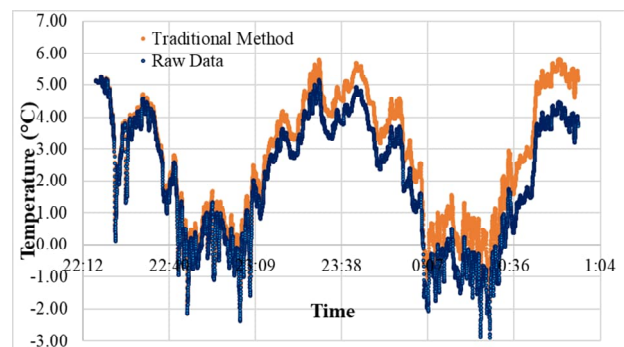


Figure 5. Comparison of car data temperatures and corrected ones using the traditional method.

However, selecting the best interpolation method is not always straightforward and significantly depends on the type and quality of the measured data. It is important to remember that there is no single optimal interpolation method (Huisman & de By, 2009). Normally, three steps are involved in selecting the best interpolation method. First is the evaluation of the data supported by their visualization. The second is to apply interpolation methods that are most suitable for both the data and the objective of the study. Finally, the results from different methods should be compared and the privileged one should be selected (Gentile et al., 2013). In this study, all three steps of selecting the best interpolation method are performed.

In the case of trend surface fitting (or global trend), simple planar surface represented a better interpolation with regard to the bilinear saddle, especially for the data which are far from the fixed stations. For those data, global trend performs an extrapolation of the values. The extrapolation of data and applying especially the bilinear saddle, creates significant errors (i.e., the two peaks occurred at the time 22:55 and 00:20 – see Figure 6 – illustrate occurrence of high errors). The results of the simple planar surface interpolation are acceptable, given the correlation of 95% (Table 2). However, global interpolators do not consider the spatial structure of the data; therefore, other interpolators are also examined.

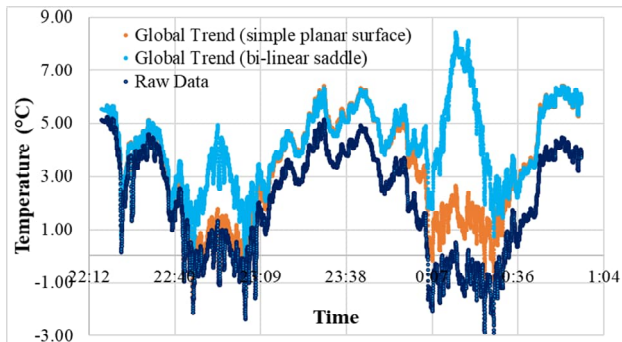


Figure 6. Mobile raw and corrected temperatures using the global trend interpolation.

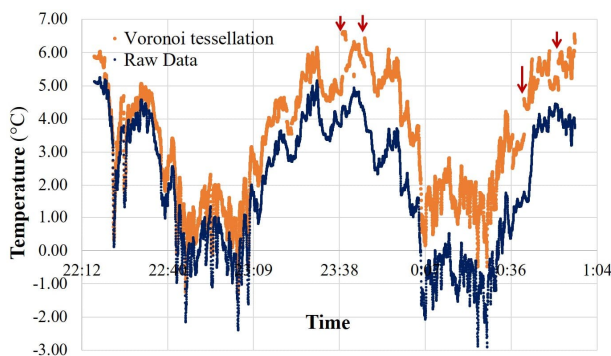


Figure 7. Mobile raw and corrected temperatures using the Voronoi Tessellation Polygons.

Using Voronoi polygons for data correction, the first thing that can be seen is the discontinuity of the corrected temperature data. This is the main problem associated with the Voronoi polygon (Gentile et al., 2013). These discontinuities are due to the fact that each polygon has its regression to be applied to the original temperature data. As a result, when moving from one polygon to its adjacent one (i.e., the boundaries), we observe an abrupt change. These changes may not be considered, but in this case and for some points they are quite high (Figure 7). For instance, the biggest jump occurred at 23:39:26 and when passing from station *wg1* to *a1* with an amount of 1.28 °C. At the time 23:40:32, 23:43:15, 23:43:21, 23:46:53, 00:36:27, 00:40:17, 00:43:00, 00:48:50, and 00:51:50, the changes were around 1 °C, and the other jumps were less than 1°C. The lowest change occurred when passing from station *mn3* to *wg10* and at the time of 23:13:50 (0.02°C). The car did not pass through the area of influence of stations *wg2*, *wg9*, *wg11*, *wg12*, and *wg14*. However, at least, part of the path goes inside the area of influence of the other stations. A correlation of 98% are achieved between the corrected and raw temperatures (Table 2). However, the mentioned discontinuities appearing in the

interpolated temperatures make the Voronoi polygons an unsuitable method of interpolation for this study.

Table 2. The correlation between corrected temperatures from different interpolation methods and raw mobile temperature data.

| MODEL | CORRELATION |
|--------------------------------------|-------------|
| TRADITIONAL METHOD | 0.978 |
| VORONOI TESSELLATION | 0.936 |
| GLOBAL TREND (SIMPLE PLANAR SURFACE) | 0.951 |
| GLOBAL TREND (BILINEAR SADDLE) | 0.508 |
| TINS | 0.831 |
| IDW | 0.962 |
| KRIGING | 0.989 |

As for the TIN interpolation, the generated surface does not cover all the data from the car path, because it is limited by the concave hull of the stations. Therefore, only part of the transect can be corrected. This is visible in Figure 8, where there is no data (discontinuities) in some parts of the corrected temperature curve. It can be considered as a drawback since the corrected temperatures of all the data cannot be achieved. It could be fixed if other measurement points (fixed stations) were present in the suburb of the city. Another problem is associated with the shape of the triangles. Some of them are extremely stretched so they cannot be considered optimal triangles. It is because the number of fixed stations is low, and they are not located perfectly in the studied area. These issues make the TINs interpolation method unsuitable to be used in the correction procedure of the mobile temperature data despite of good correlation of 83% between corrected and raw data (Table 2).

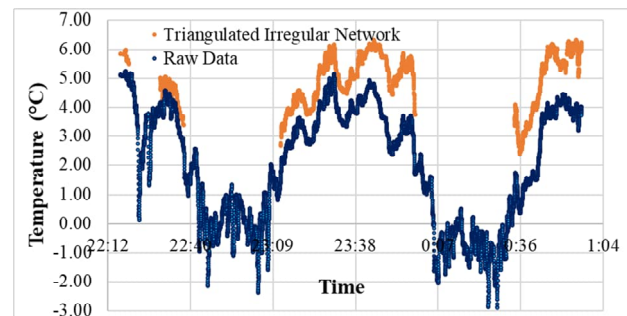


Figure 8. Mobile raw and corrected temperatures using the TINs.

The result of IDW interpolation is graphed in Figure 9. The corrected temperature curve follows the trend of the original temperature data, and there are no gaps nor sudden jumps or drops in the corrected temperatures. The correlation between the corrected and raw thermal data is 96%, which is slightly higher than the traditional method (Table 2). Although this model could be the one, Kriging interpolation is performed as well (Figure 10). The concept of Kriging is similar to IDW which uses weighting factors for the surrounding measured points to approximate the unknown value. However, another factor that is considered in Kriging is the overall spatial arrangement of the measured points and the spatial correlation between their values (Huisman & de By, 2009). The result gives the best correlation coefficient of 99% (Table 2). It can be seen that Kriging shows

a better interpolation in comparison to the other methods, since its value is closer to the raw data at the start, where the correction is expected to be zero. Indeed, at the beginning of the survey, temperature differences between raw and corrected by IDW and Kriging are 0.75°C and 0.24°C, respectively (Figures 9 and 10). Ordinary Kriging has the advantages of doing the prediction based on a spatial statistical analysis, being the best linear unbiased estimator; it is applicable to various data sets (i.e., different Kriging models is available), also sparse ones (since it automatically accounts for clustering and screening effects), and it has the capacity to consider variation bias toward specific directions and to quantify interpolation errors (Gentile et al., 2013). Kriging is therefore selected, considering its advantages and especially as it can perform a good interpolation with a low number of data (i.e., the number of fixed stations based on which mobile temperature correction was carried out, was 20). Considering the study area, which is larger than 60 km², and also the fact that almost all the fixed stations are located in the city center, Kriging appears to be the best interpolation method among all the interpolation methods for the temperature data of this study.

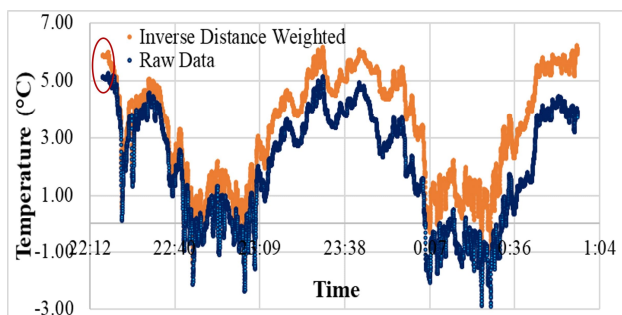


Figure 9. Mobile raw and corrected temperatures using the IDW.

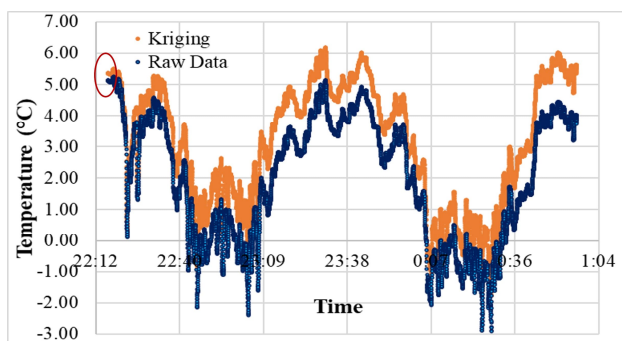


Figure 10. Mobile raw and corrected temperatures using Kriging.

In addition, when compared with the raw data from the car, the divergence of the corrected temperatures using Kriging increases over time. At the beginning of the survey (22:16:15), it is approximately 0.75 °C, whilst it is around 2.60 °C at the end of the trip (00:57:21). This is expected, as the method intends correcting the decreasing trend during nighttime. However, the last corrected temperature is not exactly equal to the first one (they are 5.35 °C and 5.37 °C, respectively, and start and end point of the transect is the same). This behavior, which is actually observed for all the interpolation method, may be explained by the accumulation of the interpolation errors, since polynomial regression degree-two was used (Equation 2). However, this residual error is negligible considering the overall precision of the adopted methodology.

4. CONCLUSION

The presence of an adequate number of weather stations, together with the data achieved from the fixed and mobile thermometers, allowed to perform a thermal study over the city of Bologna with the purpose of studying the urban microclimate. The nocturnal temperature measurement of the city center showed a considerable difference compared to its suburban area. It proved the presence of UHI phenomenon and the need for mitigation and adaptation strategies to reduce the UHI effects towards a more resilient city. High resolution mobile temperature measurements were acquired by an equipped car. The UHI is clearly visible looking just at the raw mobile temperatures. These data were then corrected using thermal data acquired from 15 weather stations and five thermometers placed in different parts of the city center. First, a second order polynomial is used to model the thermal trends of the fixed temperatures. This regression model has coefficients which are different for the various fixed stations. Then, the mobile temperatures are corrected using a traditional method as well as different interpolation methods, such as Voronoi tessellation, global trend, TINs, IDW and Kriging. Kriging interpolation model, which properly accounts for the spatial structure, showed the best performance with a correlation of 99%.

If the urban development continues in the same way as it has been until now, more frequent occurrences of heat stresses and extreme climate events would be expected. UHI is a very good indicator for urban sustainability, public health, and energy efficiency. Therefore, thermal studies of the city are essential to develop a better understanding of the city's thermal anomalies and to provide the optimal measures of tackling those (i.e., mitigation methods such as the use of green roofs and lighter-colored surfaces in urban areas, which reflect more sunlight and absorb less heat).

5. REFERENCES

- Africani, P., Bitelli, G., Lambertini, A., Minghetti, A., & Paselli, E. (2013). Integration of LIDAR data into a municipal GIS to study solar radiation. *Int. Arch. Photogramm. Remote Sens. Spat. Inf. Sci.*, 1-6.
- Bahi, H., Mastouri, H., & Radoine, H. (2020). Review of methods for retrieving urban heat islands. *Materials Today: Proceedings*, 27, 3004-3009.
- Bitelli, G., Mandanici, E., & Girelli, V. A. (2020). Multi-scale remote sensed Thermal Mapping of Urban Environments: Approaches and issues. *Communications in Computer and Information Science*, Springer, 1246, Springer, 375-386.
- Bitelli, G., Girelli, V. A., & Lambertini, A. (2018). Integrated Use of Remote Sensed Data and Numerical Cartography for the Generation of 3D City Models. *International Archives of the Photogrammetry, Remote Sensing & Spatial Information Sciences*, 42(2).
- Declet-Barreto, J., Knowlton, K., Jenerette, G. D., & Buyantuev, A. (2016). Effects of urban vegetation on mitigating exposure of vulnerable populations to excessive heat in Cleveland, Ohio. *Weather, Climate, and Society*, 8(4), 507-524.

Deilami, K., Kamruzzaman, M., & Liu, Y. (2018). Urban heat island effect: A systematic review of spatio-temporal factors, data, methods, and mitigation measures. *International journal of applied earth observation and geoinformation*, 67, 30-42.

Gentile, M., Courbin, F., & Meylan, G. (2013). Interpolating point spread function anisotropy. *Astronomy & Astrophysics*, 549, A1.

Georgiadis, T. (2017). Urban climate and risk. Oxford Handbook Topics in Physical Sciences, Oxford University Press.

Haashemi, S., Weng, Q., Darvishi, A., & Alavipanah, S. K. (2016). Seasonal variations of the surface urban heat island in a semi-arid city. *Remote Sensing*, 8(4), 352.

Huisman, O., & de By, R. A. (2009). Principles of geographic information systems. *ITC Educational Textbook Series*, 1, 17.

Imhoff, M. L., Zhang, P., Wolfe, R. E., & Bounoua, L. (2010). Remote sensing of the urban heat island effect across biomes in the continental USA. *Remote sensing of environment*, 114(3), 504-513.

Nardino, M., Cremonini, L., Georgiadis, T., Mandanici, E., & Bitelli, G. (2021). Microclimate classification of Bologna (Italy) as a support tool for urban services and regeneration. *International Journal of Environmental Research and Public Health*, 18(9), 4898.

Oke, T. R. (1982). The energetic basis of the urban heat island. *Quarterly journal of the royal meteorological society*, 108(455), 1-24.

Rumsey, D. J. (2021). *Statistics II for dummies*. John Wiley & Sons.

Taheri Shahraiyini, H., Sodoudi, S., El-Zafarany, A., Abou El Seoud, T., Ashraf, H., & Krone, K. (2016). A comprehensive statistical study on daytime surface urban heat island during summer in urban areas, case study: Cairo and its new towns. *Remote Sensing*, 8(8), 643.

Trevisiol, F., Lambertini, A., Franci, F., & Mandanici, E. (2022). An object-oriented approach to the classification of roofing materials using very high-resolution satellite stereopairs. *Remote Sensing*, 14(4), 849.

Ventura, F., Gaspari, N., Piana, S., & Rossi Pisa, P. (2010). Evolution of the Urban Heat Island of the city of Bologna (Italy) in the last 30 years. EGU General Assembly Conference Abstracts.

Zauli Sajani, S., Tibaldi, S., Scotto, F., & Lauriola, P. (2008). Bioclimatic characterisation of an urban area: a case study in Bologna (Italy). *International journal of biometeorology*, 52, 779-785.